

# Efficient Low-Rank Matrix Learning by Factorizable Nonconvex Regularization

Yaqing Wang<sup>1</sup> Quanming Yao<sup>2</sup> James T. Kwok<sup>3</sup>

<sup>1</sup>Baidu Research (Beijing), <sup>2</sup>4Paradigm Inc (Hong Kong)

<sup>3</sup>Department of Computer Science, Hong Kong University of Science and Technology

## Abstract

Matrix learning is at the core of many machine learning problems. To encourage a low-rank matrix solution, besides using the traditional convex nuclear norm regularizer, a popular recent trend is to use nonconvex regularizers that adaptively penalize singular values. They offer better recovery performance, but require computing the expensive singular value decomposition (SVD) in each iteration. To remove this bottleneck, we consider the "nuclear norm minus Frobenius norm" regularizer. Besides having nice theoretical properties on recovery and shrinkage as the other nonconvex regularizers, it can be reformulated into a factored form that can be efficiently optimized by gradient-based algorithms while avoiding the SVD computations altogether. Extensive low-rank matrix completion experiments on a number of synthetic and real-world data sets show that the proposed method obtains state-of-the-art recovery performance and is much more efficient than existing low-rank convex / nonconvex regularization and matrix factorization algorithms.

## 1 Introduction

Matrix learning is a fundamental tool in machine learning [1, 9, 23, 34]. It has been widely used on a number of tasks such as matrix completion [9], robust principal component analysis [6], multitask learning [10] and subspace clustering [24]. To avoid the problem to be ill-posed, the target matrix is often assumed to have a low rank [7]. However, rank minimization is NP-hard [7]. Thus, computationally, a more feasible approach is to use a regularizer that encourages the target matrix to be low-rank. A popular choice is nuclear norm regularizer, defined as the sum of singular values, which is the tightest convex surrogate of the matrix rank [7]. There also exist various nonconvex low-rank regularizers (Table 1). Schatten- $p$  norm [28, 33] serves as better surrogates for rank which enforces  $\ell_p$  ( $0 < p < 1$ ) on the vector of singular values. Truncated  $\ell_{1-2}$  norm [26] is an unbiased regularizer with properly chosen hyperparameter. Apart from them, based on the intuition that larger singular values carry more information and thus should be protected, adaptive nonconvex low-rank regularizers emerge. Common examples include the capped- $\ell_1$  penalty [41], log-sum penalty (LSP) [9], and minimax concave penalty (MCP) [40]. Empirically, they obtain much better recovery performance than other low-rank regularizers including both the convex nuclear norm regularizer and the nonconvex Schatten- $p$  norm. Theoretically, they also offer better statistical recovery guarantees than the convex nuclear norm [16].

Scalability is the bottleneck of using these low-rank regularizers. Formulated as a function of singular values, aforementioned low-rank regularizers require computing singular value decomposition (SVD) in each iteration of the optimization process. However, SVD computation scales cubically with the matrix size, which is expensive on large matrices. Therefore, factored low-rank regularizers are invented to avoid SVD. The factored nuclear norm or matrix factorization [34] factorizes the recovered matrix into two factor matrices, which explicitly limits the rank of matrix. It is theoretically proved that factored nuclear norm can obtain the same result as nuclear norm as long as the dimension

Table 1: Comparisons between nonconvex low-rank regularizers on (A): Scalability (can be optimized in factored form); (B): Performance (can adaptive penalize singular values); (C): Statistical guarantee; (D): Convergence guarantee.

nonconvex low-rank regularizer	expression	(A)	(B)	(C)	(D)
factored nuclear [34]	$\min_{\mathbf{X}=\mathbf{WH}^\top} \frac{\lambda}{2} (\ \mathbf{W}\ _F^2 + \ \mathbf{H}\ _F^2)$	✓	✗	✓	✓
Schatten-p [28]	$\lambda (\sum_{i=1}^m \sigma_i^p(\mathbf{X}))^{1/p}$	✗	✗	✓	✓
factored group-sparse regularizer [12]	$\min_{\mathbf{X}=\mathbf{WH}^\top} \frac{\lambda}{2} (\ \mathbf{W}\ _{2,1} + \ \mathbf{H}^\top\ _{2,1})$	✓	✗	✓	✓
capped- $\ell_1$ [41], LSP [9], and MCP [40]	$\lambda \sum_{i=1}^m \hat{r}(\sigma_i(\mathbf{X}))$ (see $\hat{r}$ in Table 2 [32])	✗	✓	✓	✓
truncated $\ell_{1-2}$ [26]	$\sum_{i=t+1}^n \sigma_i(\mathbf{X}) - (\sum_{i=t+1}^n \sigma_i^2(\mathbf{X}))^{1/2}$	✗	✓	✓	✓
NNFN	$\ \mathbf{X}\ _* - \ \mathbf{X}\ _F$	✗	✓	✓	✓
factored NNFN	$\min_{\mathbf{X}=\mathbf{WH}^\top} \frac{\lambda}{2} (\ \mathbf{W}\ _F^2 + \ \mathbf{H}\ _F^2) - \lambda \ \mathbf{WH}^\top\ _F$	✓	✓	✓	✓

of the factor matrices are properly set [34]. Then many works endeavor to theoretically justify the factored nuclear norm [35, 37]. While some other works target at analyzing suitable algorithms to optimize the problem with factored nuclear norm such as gradient descent with implicit regularization [17] and Riemannian preconditioning [36, 2].

For nonconvex low-rank regularizers, only Schatten-p norm can be approximated and scaled by the factored group-sparse regularization [12]. While adaptive nonconvex low-rank regularizers, which obtain state-of-the-art recovery performance, existing ones cannot be factorized due to complicated forms with explicit access to individual singular values. This makes subsequent optimization problems more difficult and computationally inefficient. Consequently, this limits the application scenario of adaptive nonconvex low-rank regularizers.

In this paper, we propose a scalable adaptive nonconvex regularizer. Specifically, our contribution can be summarized as follows:

- We propose a new adaptive nonconvex regularizer called the nuclear norm minus Frobenius norm regularizer. We provably identify the adaptive shrinkage property of this regularizer. We propose a proximal algorithm to solve the resultant matrix learning problem, with proved statistical guarantee under the restricted isometry property.
- Further, we show that this new regularizer can be factorized for scalability, which sidesteps the expensive SVD. This problem can be optimized by general algorithm such as gradient descent. We also prove statistical guarantee and convergence guarantee under the restricted isometry property.
- Extensive experiments are performed on an important class of low-rank matrix learning problems, namely matrix completion [?, 7]. A number of synthetic and real-world recommendation / hyperspectral / climate data sets are used. Results consistently show that the proposed algorithm obtains state-of-the-art recovery performance as the other adaptive nonconvex regularizers, but can be orders of magnitude faster on large data sets.

**Notations:** In the sequel, vectors are denoted by lowercase boldface, matrices by uppercase boldface, and the transpose by the superscript  $(\cdot)^\top$ . For a vector  $\mathbf{x} = [x_i] \in \mathbb{R}^m$ ,  $\text{Diag}(\mathbf{x})$  constructs a  $m \times m$  diagonal matrix with the  $i$ th diagonal element being  $x_i$ .  $\mathbf{I}$  denotes the identity matrix. For a square matrix  $\mathbf{X}$ ,  $\text{tr}(\mathbf{X})$  is its trace. For matrix  $\mathbf{X} \in \mathbb{R}^{m \times n}$  (without loss of generality, we assume that  $m \geq n$ ),  $\|\mathbf{X}\|_F = \sqrt{\text{tr}(\mathbf{X}^\top \mathbf{X})}$  is its Frobenius norm. Let the singular value decomposition (SVD) of  $\mathbf{X}$  be  $\mathbf{U} \text{Diag}(\boldsymbol{\sigma}(\mathbf{X})) \mathbf{V}^\top$ , where  $\mathbf{U} \in \mathbb{R}^{m \times k^*}$ ,  $\mathbf{V} \in \mathbb{R}^{n \times k^*}$ ,  $k^*$  is the rank of  $\mathbf{X}$ ,  $\boldsymbol{\sigma}(\mathbf{X}) = [\sigma_i(\mathbf{X})] \in \mathbb{R}^{k^*}$  with  $\sigma_i(\mathbf{X})$  being the  $i$ th singular value of  $\mathbf{X}$  and  $\sigma_1(\mathbf{X}) \geq \sigma_2(\mathbf{X}) \geq \dots \geq \sigma_{k^*}(\mathbf{X}) \geq 0$ .

## 2 Background: Low-Rank Matrix Learning

As minimizing the rank is NP-hard [7], low-rank matrix learning is often formulated as the following optimization problem:

$$\min f(\mathbf{X}) + \lambda r(\mathbf{X}), \quad (1)$$

where  $f$  is a smooth function (usually the loss),  $r(\mathbf{X})$  is a regularizer that encourages  $\mathbf{X}$  to be low-rank, and  $\lambda \geq 0$  is a tradeoff hyperparameter.

## 2.1 Convex Nuclear Norm Regularizer

The most popularly used low-rank regularizer is based on the nuclear norm  $\|\mathbf{X}\|_* = \|\boldsymbol{\sigma}(\mathbf{X})\|_1$  [7], which is also the tightest convex surrogate of the matrix rank [13]. Problem (1) is usually solved by the proximal algorithm [30]. At the  $t$ th iteration, it generates the next iterate by computing the proximal step  $\mathbf{X}_{t+1} = \text{prox}_{\eta\lambda r}(\mathbf{X}_t - \eta\lambda\nabla(\mathbf{X}_t))$ , where  $\eta > 0$  is the stepsize, and  $\text{prox}_{\lambda r}(\mathbf{Z}) = \arg \min_{\mathbf{X}} \frac{1}{2}\|\mathbf{X} - \mathbf{Z}\|_2^2 + \lambda r(\mathbf{X})$  is the proximal operator. In general, the proximal operator should be easily computed. For the nuclear norm, its proximal operator is computed as [5]:

$$\text{prox}_{\lambda\|\cdot\|_*}(\mathbf{Z}) = \mathbf{U}(\text{Diag}(\boldsymbol{\sigma}(\mathbf{Z})) - \lambda\mathbf{I})_+ \mathbf{V}^\top, \quad (2)$$

where  $\mathbf{U}\text{Diag}(\boldsymbol{\sigma}(\mathbf{Z}))\mathbf{V}^\top$  is the singular value decomposition (SVD) of  $\mathbf{Z}$ , and  $\mathbf{A}_+ = [\max(A_{ij}, 0)]$ .

## 2.2 Nonconvex Regularizers

Recently, various nonconvex regularizers appear (Table 1). Albeit all being nonconvex, the targets of these nonconvex regularizers are different. Schatten- $p$  norm [33] can act as a better surrogate for rank. Truncated  $\ell_{1-2}$  regularizer [26], which keeps the  $t$  largest singular values of the matrix argument intact and only penalizes the remaining ones, is unbiased in the sense that  $\ell_{t,1-2}(\boldsymbol{\sigma}(\mathbf{X})) = 0$  if and only if  $\mathbf{X}$  has rank  $t + 1$  [26]. In this paper, we focus on a adaptive nonconvex regularizers. Common examples include the capped- $\ell_1$  penalty [41], log-sum penalty (LSP) [9], and minimax concave penalty (MCP) [40]. They can be written in the general form of

$$r(\mathbf{X}) = \sum_{i=1}^n \hat{r}(\sigma_i(\mathbf{X})), \quad (3)$$

where  $\hat{r}(\alpha)$  is nonlinear, concave and non-decreasing for  $\alpha \geq 0$  with  $\hat{r}(0) = 0$ . In contrast to the proximal operator in (2) which penalizes all singular values of  $\mathbf{Z}$  by the same amount  $\lambda$ , adaptive nonconvex regularizers penalize less on the larger singular values which are more informative. They outperform the (convex) nuclear norm regularizer on many low-rank matrix learning applications such as image inpainting [15], collaborative filtering [25] and background modeling [39] empirically. Moreover, it can be shown theoretically that they obtain lower recovery errors than the nuclear norm regularizer [9, 40, 41, 16]. However, learning with nonconvex regularizers is very difficult. It usually requires dedicated solvers to leverage special structures (such as the low-rank-plus-sparse structure in [19, 39]) or involves several iterative algorithms (such as the difference of convex functions algorithm (DCA) [20] with subproblems solved by the alternating direction method of multipliers (ADMM) [3] for truncated  $\ell_{1-2}$  regularized problem). This computation bottleneck limits their applications in practice.

## 2.3 Factored Regularizers

Note that aforementioned regularizers require access to individual singular values. As computing the singular values of a  $m \times n$  matrix (with  $m \geq n$ ) via SVD takes  $O(mn^2)$  time, this can be costly for a large matrix. Even when rank- $k$  truncated SVD is used, the computation cost is still  $O(mnk)$ , and can be problematic when both  $m$  and  $n$  are large. To relieve the computational burden, factored low-rank regularizers are invented to avoid SVD. Nuclear norm can be rewritten in a factored form [34, 38, 36, 2, 35, 37, 17] that does not require accessing the singular values and hence avoids using SVD. For a matrix  $\mathbf{X}$  with rank  $k^* \leq k$ ,  $\|\mathbf{X}\|_* = \min_{\mathbf{X}=\mathbf{W}\mathbf{H}^\top} \frac{1}{2}(\|\mathbf{W}\|_F^2 + \|\mathbf{H}\|_F^2)$ , where  $\mathbf{W} \in \mathbb{R}^{m \times k}$  and  $\mathbf{H} \in \mathbb{R}^{n \times k}$ . As for nonconvex low-rank regularizers, only Schatten- $p$  norm can be optimized in factored form [33, 12]. Other nonconvex regularizers need to penalize individual singular values, and so cannot be written in the factored form.

## 3 Nuclear Norm Minus Frobenius Norm Regularizer

In this paper, we propose a scalable adaptive nonconvex regularizer

$$r_{\text{NNFN}}(\mathbf{X}) = \|\mathbf{X}\|_* - \|\mathbf{X}\|_F, \quad (4)$$

which will be called the ‘‘nuclear norm minus Frobenius norm’’ (NNFN) regularizer in the sequel. In Section 3.1, we first provably show NNFN regularizer shares the adaptive shrinkage property with existing adaptive nonconvex regularizers. Moreover, as described in Section 3.2, this regularizer can be written in factored form which bypasses the necessity of performing SVD in each iteration.

### 3.1 Adaptive Shrinkage Property

Here, we show the NNFN regularizer provably satisfies adaptive shrinkage of the singular values when used with a proximal algorithm. First, the following Proposition<sup>1</sup> shows that the proximal operator of  $r_{\text{NNFN}}(\cdot)$  can be easily obtained from the corresponding proximal operator  $\text{prox}_{\lambda\|\cdot\|_{1-2}}(\cdot)$  of the  $\ell_{1-2}$  regularizer.

**Proposition 3.1.** *Given a matrix  $\mathbf{Z}$ , let its SVD be  $\bar{\mathbf{U}}\text{Diag}(\boldsymbol{\sigma}(\mathbf{Z}))\bar{\mathbf{V}}^\top$ , and  $\lambda \leq \|\boldsymbol{\sigma}(\mathbf{Z})\|_\infty$ .*

$$\text{prox}_{\lambda r_{\text{NNFN}}}(\mathbf{Z}) = \bar{\mathbf{U}}\text{Diag}(\text{prox}_{\lambda\|\cdot\|_{1-2}}(\boldsymbol{\sigma}(\mathbf{Z})))\bar{\mathbf{V}}^\top, \quad (5)$$

where  $\text{prox}_{\lambda\|\cdot\|_{1-2}}(\mathbf{z}) = \bar{\mathbf{z}}(\|\bar{\mathbf{z}}\|_2 + \lambda)/\|\bar{\mathbf{z}}\|_2$  with  $\bar{\mathbf{z}} = \text{prox}_{\lambda\|\cdot\|_1}(\mathbf{z}) = \text{sign}(\mathbf{z}) \odot \max(|\mathbf{z}| - \lambda, 0)$  being the soft thresholding operator [11].

As is well-known, the soft thresholding operator leads to a sparse  $\text{prox}_{\lambda\|\cdot\|_{1-2}}(\boldsymbol{\sigma}(\mathbf{Z}))$ , and so  $\text{prox}_{\lambda r_{\text{NNFN}}}(\mathbf{Z})$  is low-rank. Recall from (2) that the proximal operator of the nuclear norm equally penalizes each singular value by  $\lambda$  until it reaches zero. The following Proposition shows that  $\text{prox}_{\lambda r_{\text{NNFN}}}(\cdot)$  adaptively shrinks the singular values of its matrix argument, in that larger singular values are penalized less.

**Proposition 3.2** (Adaptive Shrinkage Property). *Let  $\tilde{\boldsymbol{\sigma}} = [\tilde{\sigma}_i] = \text{prox}_{\lambda\|\cdot\|_{1-2}}(\boldsymbol{\sigma}(\mathbf{Z}))$  in (5). Then, (i)  $\sigma_i(\mathbf{Z}) \geq \tilde{\sigma}_i$  (shrinkage); and (ii)  $\sigma_i(\mathbf{Z}) - \tilde{\sigma}_i \leq \sigma_{i+1}(\mathbf{Z}) - \tilde{\sigma}_{i+1}$  (adaptivity), where strict inequality holds at least for one  $i$ .*

This property is important for obtaining good empirical performance [15, 21]. The following Corollary shows that existing adaptive nonconvex regularizers of the form in (3) all share this property. Other nonconvex regularizers such  $\ell_{t,1-2}$  and Schatten- $p$  norm, do not have this property due to the lack of analytic expressions.

**Corollary 3.3.** *The two properties in Proposition 3.2 also hold for the proximal operators of the other nonconvex low-rank regularizers of the form in (3).*

Figure 1 shows the shrinkage performed by adaptive nonconvex regularizers versus the convex nuclear norm regularizer. As can be seen, the convex nuclear norm regularizer shrinks all singular values by the same amount; whereas the adaptive nonconvex regularizers enforce different amounts of shrinkage depend on the magnitude of  $\sigma_i(\mathbf{Z})$ .

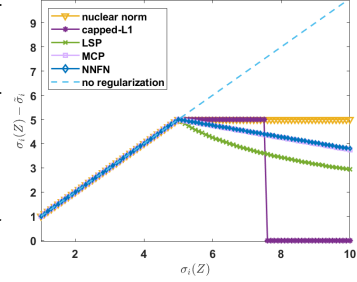


Figure 1: Shrinkage on singular values performed by different regularizers. The hyperparameters are tuned such that  $\tilde{\sigma}_i$  is zero for  $\sigma_i(\mathbf{Z}) \leq 5$ .

### 3.2 Solving Problem (1) with NNFN Regularizer

With the simple proximal operator obtained in Proposition 3.1, learning with the NNFN regularizer can be readily solved with the proximal algorithm. Thus in Section 3.2.1, we first introduce a direct use of proximal algorithm based on Proposition 3.1, which still relies on computing the SVD in each iteration. In Section 3.2.2, we present a simple and scalable algorithm that avoids SVD computations by using a factored NNFN regularizer.

**Algorithm 1** Solving problem (1) with NNFN regularizer.

**Input:** Randomly initialized  $\mathbf{X}^0$ , stepsize  $\eta$ ;  
1: **for**  $t = 1, \dots, T$  **do**  
2:   obtain  $\mathbf{Z}^t = \mathbf{X}^{t-1} - \eta \nabla f(\mathbf{X}^{t-1})$ ;  
3:   update  $\mathbf{X}^t$  as  $\text{prox}_{\lambda r_{\text{NNFN}}}(\mathbf{Z}^t)$ ;  
4: **end for**  
5: **return**  $\mathbf{X}^T$ .

**Algorithm 2** Solving problem (1) with factored NNFN regularizer.

**Input:** Randomly initialized  $\mathbf{W}^0, \mathbf{H}^0$ , stepsize  $\eta$ ;  
1: **for**  $t = 1, \dots, T$  **do**  
2:   update  $\mathbf{W}^t = \mathbf{W}^{t-1} - \eta \nabla_{\mathbf{W}} F(\mathbf{W}^t, \mathbf{H}^t)$ ;  
3:   update  $\mathbf{H}^t = \mathbf{H}^{t-1} - \eta \nabla_{\mathbf{H}} F(\mathbf{W}^t, \mathbf{H}^t)$ ;  
4: **end for**  
5: **return**  $\mathbf{X}^T = \mathbf{W}^T (\mathbf{H}^T)^\top$ .

<sup>1</sup>All the proofs are in Appendix A.

### 3.2.1 Naive Solver by Proximal Algorithm

We first present a direct application of the proximal algorithm to problem (1) with the NNFN regularizer. At the  $t$ th iteration, we obtain  $\mathbf{Z}^t = \mathbf{X}^{t-1} - \eta \nabla f(\mathbf{X}^{t-1})$ , and then perform the proximal step in Proposition 3.1. The complete procedure, is shown in Algorithm 1.

Existing theoretical analysis [16] for adaptive nonconvex regularizer does not apply for our NNFN regularizer, as it requires access to individual singular values, while our regularizer is not separable. In the following, we establish statistical guarantee based on Restricted Isometry Property (RIP) [8] introduced below.

**Definition 1** (Restricted Isometry Property (RIP) [8]). *An affine transformation  $\mathcal{A}$  satisfies RIP if for all  $\mathbf{X} \in \mathbb{R}^{m \times n}$  of rank at most  $k$ , there exists a constant  $\delta_k \in (0, 1)$  such that:*

$$(1 - \delta_k) \|\mathbf{X}\|_F^2 \leq \|\mathcal{A}(\mathbf{X})\|_2^2 \leq (1 + \delta_k) \|\mathbf{X}\|_F^2. \quad (6)$$

Under the RIP condition, we prove in the following that stable recovery is guaranteed where the estimation error depends linearly on  $\|\mathbf{e}\|_2^2$ . In [26], they obtain comparable recovery error for truncated  $\ell_{1-2}$  regularizer with arbitrary  $t$ , which is consistent with our analysis.

**Theorem 3.4** (Stable Recovery). *With  $f(\mathbf{X}) = \frac{1}{2} \|\mathcal{A}(\mathbf{X}) - \mathbf{b}\|_2^2$ , where  $\mathcal{A}$  is an affine transform satisfying the RIP with  $\delta_{2k} \leq 1/3$ , and  $\mathbf{b} = \mathcal{A}(\mathbf{X}^*) + \mathbf{e}$  is a measurement vector corresponding to a rank- $k^*$  matrix  $\mathbf{X}^*$  and error vector  $\mathbf{e}$ . Consider the equivalent constrained formulation of (7):  $\arg \min_{\mathbf{W}, \mathbf{H}} f(\mathbf{W}\mathbf{H}^\top)$  s.t.  $\frac{1}{2}(\|\mathbf{W}\|_F^2 + \|\mathbf{H}\|_F^2) - \|\mathbf{W}\mathbf{H}^\top\|_F \leq \beta'$ , where  $\beta' \geq 0$  is a hyperparameter. Assume that the sequence  $\{\mathbf{X}^t\}$  satisfying  $f(\mathbf{X}^{t+1}) < f(\mathbf{X}^t)$ . The recovery error is bounded as  $\|\mathbf{X}^t - \mathbf{X}^*\|_F^2 \leq \frac{(c_1+1)^2(c_1^2+\epsilon)\|\mathbf{e}\|_2^2}{c_1^2(1-\delta_{2k^*})}$  for sufficiently large  $t$  and some universal constants  $c_1, \epsilon$ .*

In the following, we study its complexities. For concreteness, we consider the context of matrix completion [7], which tries to fill in the missing entries of an incomplete matrix  $\mathbf{O} \in \mathbb{R}^{m \times n}$ . We use the square loss  $f(\mathbf{X}) = \frac{1}{2} \|\mathcal{P}_\Omega(\mathbf{X} - \mathbf{O})\|_F^2$ , where  $\Omega \in \{0, 1\}^{m \times n}$  is the set denoting positions of the observed entries (with  $\Omega_{ij} = 1$  if  $O_{ij}$  is observed, and 0 otherwise), and  $\mathcal{P}_\Omega(\cdot)$  is the projection operator such that  $[\mathcal{P}_\Omega(\mathbf{A})]_{ij} = A_{ij}$  if  $\Omega_{ij} = 1$  and 0 otherwise. As can be easily seen, the iteration time complexity of Algorithm 1 is dominated by SVD. Let  $r_t$  (with  $n \geq r_t \geq k$ ) be the rank estimated at the  $t$ th iteration. We perform rank- $k$  truncated SVD, which reduces the time complexity from  $O(mn^2)$  to  $O(mnk)$ . Its space complexity is  $O(mn)$ , as the complete matrix  $\mathbf{X}$  has to be kept.

### 3.2.2 Scalable and General Solver for the Factored Regularizer

In this section, we propose a more efficient solver which removes the SVD bottleneck. The key observation is that the NNFN regularizer in (4) can be computed on the recovered matrix without touching singular values explicitly. The Frobenius norm of a matrix can be computed without using its singular values, and the nuclear norm can be replaced by the factored nuclear norm. With this factored NNFN regularizer, the matrix learning problem then becomes:

$$\min_{\mathbf{W}, \mathbf{H}} F(\mathbf{W}, \mathbf{H}) \equiv f(\mathbf{W}\mathbf{H}^\top) + \frac{\lambda}{2} (\|\mathbf{W}\|_F^2 + \|\mathbf{H}\|_F^2) - \lambda \|\mathbf{W}\mathbf{H}^\top\|_F. \quad (7)$$

Thus, SVD can be completely avoided. In contrast, the other nonconvex low-rank regularizers (including the very related truncated  $\ell_{1-2}$  regularizer with  $t \neq 0$ ) need to penalize individual singular values, and so cannot utilize this factored form.

The following Theorem shows that reformulating the optimization problem in factored form does not affect the recovery bound. In particular, as in Theorem 3.4, the recovery error still depends linearly on the norm of the error.

**Theorem 3.5** (Stable Recovery). *With  $f(\mathbf{X}) = \frac{1}{2} \|\mathcal{A}(\mathbf{X}) - \mathbf{b}\|_2^2$ , where  $\mathcal{A}$  is an affine transform satisfying the RIP, and  $\mathbf{b} = \mathcal{A}(\mathbf{X}^*) + \mathbf{e}$  is a measurement vector corresponding to a rank- $k^*$  matrix  $\mathbf{X}^*$  and error vector  $\mathbf{e}$ . Assume that the isometry constant of  $\mathcal{A}$  satisfies  $\delta_{2k^*} \leq 1/3$ . Consider the equivalent constrained formulation of (7):  $\arg \min_{\mathbf{W}, \mathbf{H}} f(\mathbf{W}\mathbf{H}^\top)$  s.t.  $\frac{1}{2}(\|\mathbf{W}\|_F^2 + \|\mathbf{H}\|_F^2) - \|\mathbf{W}\mathbf{H}^\top\|_F \leq \beta'$ , where  $\beta' \geq 0$  is a hyperparameter. Let  $\mathbf{X}^t = \mathbf{W}^t(\mathbf{H}^t)^\top$  and assume that the sequence  $\{\mathbf{X}^t\}$  satisfying  $f(\mathbf{X}^{t+1}) < f(\mathbf{X}^t)$ . Then,  $\|\mathbf{X}^t - \mathbf{X}^*\|_F \leq c' \|\mathbf{e}\|_2$  for some constant  $c'$  and sufficiently large  $t$ .*

Unlike other regularizers which requires dedicated solvers, the reformulated problem (7) can be simply solved by general solvers such as gradient descent. In particular, gradients of  $F(\mathbf{W}, \mathbf{H})$  can be easily obtained. Let  $\mathbf{Q} \equiv \mathbf{W}\mathbf{H}^\top \neq \mathbf{0}$ , and  $c = \lambda/\|\mathbf{W}\mathbf{H}^\top\|_F$ . Then,  $\nabla_{\mathbf{W}}F(\mathbf{W}, \mathbf{H}) = [\nabla_{\mathbf{Q}}f(\mathbf{Q})]\mathbf{H} + \lambda\mathbf{W} - c\mathbf{W}(\mathbf{H}^\top\mathbf{H})$ , and  $\nabla_{\mathbf{H}}F(\mathbf{W}, \mathbf{H}) = [\nabla_{\mathbf{Q}}f(\mathbf{Q})]^\top\mathbf{W} + \lambda\mathbf{H} - c\mathbf{H}(\mathbf{W}^\top\mathbf{W})$ . These only involve simple matrix multiplications, without any SVD computation. Moreover, we can easily replace the simple gradient descent by recent solvers with improved performance.

Although the proposed regularizer is non-smooth, the following guarantee convergence to a critical point of (7), which can be used to form a critical point of the original low-rank matrix learning problem in (1).

**Theorem 3.6** (Convergence Guarantee). *Assume that  $\mathbf{W}^t(\mathbf{H}^t)^\top \neq \mathbf{0}$  during the iterations, gradient descent on (7) can converge to a critical point  $(\bar{\mathbf{W}}, \bar{\mathbf{H}})$ . Moreover, the obtained  $\bar{\mathbf{X}} = \bar{\mathbf{W}}\bar{\mathbf{H}}^\top$  is also a critical point of (1), with  $r$  being the NNFN regularizer.*

The complete procedure is shown in Algorithm 2. As learning with the factored NNFN does not need to compute the expensive SVD, it has a much lower time complexity. Specifically, again in the context of matrix completion, multiplication of the sparse matrix  $\nabla_{\mathbf{Q}}f(\mathbf{Q}) = \mathcal{P}_{\Omega}(\mathbf{Q} - \mathbf{O})$  and  $\mathbf{H}$  in  $\nabla_{\mathbf{W}}F(\mathbf{W}, \mathbf{H})$  (and similarly multiplication of  $[\nabla_{\mathbf{Q}}f(\mathbf{Q})]^\top$  and  $\mathbf{W}$  in  $\nabla_{\mathbf{H}}F(\mathbf{W}, \mathbf{H})$ ) takes  $O(\|\Omega\|_0 k)$  time, computation of  $\mathbf{W}(\mathbf{H}^\top\mathbf{H})$ ,  $\mathbf{H}(\mathbf{W}^\top\mathbf{W})$  and  $\|\mathbf{W}\mathbf{H}^\top\|_F$  (computed as  $\sqrt{\text{tr}((\mathbf{H}^\top\mathbf{H})(\mathbf{W}^\top\mathbf{W}))}$ ) takes  $O(mk^2)$  time. Thus, the iteration time complexity is  $O(\|\Omega\|_0 k + mk^2)$ . As for space, using the factored form reduces the parameter size from  $O(mn + \|\Omega\|_0)$  to  $O(mk + \|\Omega\|_0)$ , where  $\|\Omega\|_0$  is the space for keeping the sparse matrix  $\mathbf{O}$ .

### 3.2.3 Comparison with Other Regularizers

We compare the proposed solvers with state-of-the-art solvers for other regularizers in Table 2. For space, only solvers for truncated  $\ell_{1-2}$  [26] and NNFN require keeping the complete matrix which takes  $O(mn)$  space, while the other methods have comparable and much smaller space requirements. Hence the space complexity is not included in the table.

Table 2: Comparison state-of-the-art solvers for various matrix completion methods that will be compared in Section 4. Here,  $r_t$  (usually  $\geq k$ ) is an estimated rank at the  $t$ th iteration,  $\hat{r}_t = r_t + r_{t-1}$ , and  $q$  is number of inner ADMM iterations used in [26].

regularizer	solver	time complexity
nuclear norm [7]	softimpute algorithm with alternating least squares[19]	$O(\ \Omega\ _0 k + m\hat{r}_t^2)$
factored nuclear [34]	nonlinear successive over-relaxation algorithm [38]	$O(\ \Omega\ _0 k + mk^2)$
probabilistic matrix factorization [27]	Bayesian probabilistic matrix factorization solver using Markov Chain Monte Carlo [32]	$O(\ \Omega\ _0 k^2 + mk^3)$
factored group-sparse regularizer [12]	proximal alternating linearized algorithm coupled with iteratively reweighted minimization	$O(mnk)$
capped- $\ell_1$ [41], LSP [9], and MCP [40]	a solver leveraging power method and "low-rank plus sparse" structure [39]	$O(\ \Omega\ _0 r_t + m\hat{r}_t^2)$
truncated $\ell_{1-2}$ [26]	DCA coupled with ADMM [26]	$O(qmn^2)$
NNFN	proximal algorithm	$O(mnr_t)$
factored NNFN	general solvers such as gradient descent	$O(\ \Omega\ _0 k + mk^2)$

As can be seen, only factored NNFN can be solved by general solvers such as gradient descent. This makes our method easy to use and improved. In contrast, other nonconvex regularizers are difficult to optimize and require dedicated solvers. Although the time complexity is comparable in big O, we will show in next section that learning with factored NNFN is much more scalable.

**Remark 3.1.** *Truncated  $\ell_{1-2}$  regularizer [26] is a related existing nonconvex regularizer. When  $t = 0$ , it reduces to our NNFN regularizer. However, existing solver for this truncated  $\ell_{1-2}$  regularizer is very computationally expensive, which requires the combined use of the difference of convex functions algorithm (DCA) [20] and the alternating direction method of multipliers (ADMM) [3]. In contrast, without the operation to truncate singular values, our NNFN regularizer (1) allows closed-form proximal operator while truncated  $\ell_{1-2}$  requires iterative solvers; (2) is proved to enforce*

*adaptive shrinkage while truncated  $\ell_{1-2}$  does not; (3) can be optimized in factored form without taking SVD while truncated  $\ell_{1-2}$  cannot avoid repeated SVD; Therefore, the discovery of NNFN regularizer is new and important.*

## 4 Experiments

In this section, we perform matrix completion experiments on a number of synthetic and real-world data sets, using a PC with Intel i7 3.6GHz CPU and 48GB memory. Experiments are repeated five times, and the averaged performance reported. Because of the lack of space, results on the standard deviation of the performance are shown in Appendix B.2.

### 4.1 Setup

The proposed NNFN regularizer which is solved by a direct application of proximal algorithm, and its scalable variant factored NNFN solved by gradient descent, will be compared with other regularizers and their factored variants optimized by their respective state-of-the-art solvers. The low-rank regularizers compared include: (i) convex nuclear norm regularizer  $\|\mathbf{X}\|_*$  [7], optimized by the recent softImpute algorithm via alternating least squares [19]; (ii) truncated  $\ell_{1-2}$  regularizer [26], optimized with DCA algorithm with sub-problems solved by ADMM; and (iii) adaptive nonconvex low-rank regularizers of the form (3), including the capped- $\ell_1$  penalty [41], log-sum penalty (LSP) [9]; and minimax concave penalty (MCP) [40], optimized by the low-rank matrix learning solver FaNCL [39]. Then for the factored regularizers, which solves  $\min_{\mathbf{W}, \mathbf{H}} f(\mathbf{WH}^\top) + \frac{\lambda}{2}g(\mathbf{W}, \mathbf{H})$ , we compare with (i) factored nuclear norm [34] solved by low-rank matrix fitting algorithm (LMaFit) [38]; (ii) Bayesian probabilistic matrix factorization (BPMF) [27], which is a Bayesian model trained with Markov chain Monte Carlo [14]; and (iii) factored group-sparse regularizer (factored GSR) [12] which approximates Schatten-p norm regularizer and is optimized by proximal alternating linearized minimization. All the algorithms are implemented in MATLAB (with sparse tensor and matrix operations written in C as MEX functions) and obtained from the respective authors. Each algorithm is stopped when the relative difference between objective values in consecutive iterations is smaller than  $10^{-4}$ . All hyperparameters including  $\lambda$ ,  $k$ , and  $r_t$  hyperparameters required by compared methods and stepsize are tuned by grid search using the validation set. More details are in Appendix B.1.

Given a partially observed matrix  $\mathbf{O}$ , let  $\Omega^\perp$  be the matrix indexing positions of the unobserved elements (i.e.,  $\Omega_{ij}^\perp = 0$  if  $O_{ij}$  is observed, and 1 otherwise), and  $\tilde{\mathbf{X}}$  be the matrix recovered. Following [31, 39], performance on the synthetic data is measured by the normalized mean squared error (NMSE) on  $\Omega^\perp$ :  $\text{NMSE} = \|\mathcal{P}_{\Omega^\perp}(\tilde{\mathbf{X}} - \mathbf{G})\|_F / \|\mathcal{P}_{\Omega^\perp}(\mathbf{G})\|_F$ , where  $\mathbf{G}$  is the ground-truth matrix. On the real-world data sets, we use the root mean squared error (RMSE) on  $\Omega^\perp$ :  $\text{RMSE} = (\|\mathcal{P}_{\Omega^\perp}(\tilde{\mathbf{X}} - \mathbf{O})\|_F^2 / \|\Omega^\perp\|_0)^{1/2}$ . Besides the error, we also report the training time in seconds. Due to the lack of space, rank of the recovered matrix is reported in Appendix B.2.

### 4.2 Synthetic Data

First,  $\mathbf{W}, \mathbf{H} \in \mathbb{R}^{m \times k^*}$  are generated with elements sampled i.i.d. from the standard normal distribution  $\mathcal{N}(0, 1)$ . We set  $k^* = 5$ , and vary  $m$  in  $\{500, 1000, 2000\}$ . The  $m \times m$  ground-truth matrix (with rank  $k^*$ ) is then constructed as  $\mathbf{G} = \mathbf{WH}^\top$ . The observed matrix  $\mathbf{O}$  is generated by adding noise matrix  $\mathbf{E}$  to  $\mathbf{G}$ :  $\mathbf{O} = \mathbf{G} + \mathbf{E}$ . The elements of  $\mathbf{E}$  are sampled from  $\mathcal{N}(0, 0.1)$ . A set of  $\|\Omega\|_0 = 2mk^* \log(m)$  random elements in  $\mathbf{O}$  are observed. 50% of them are randomly sampled for training, and the rest is taken as validation set for hyperparameter tuning. We define the sparsity ratio  $s$  of the observed matrix as its fraction of observed elements (i.e.,  $s = \|\Omega\|_0 / m^2$ ).

#### 4.2.1 Recovery Performance

Table 3 shows the results. As can be seen, nonconvex regularizers (including the proposed  $r_{\text{NNFN}}$ ) consistently yield better recovery performance. Among the nonconvex regularizers, all of them yield comparable errors. As for the rank (reported in Appendix B.2), all methods (except the nuclear norm regularizer) can recover the true rank. As for speed, factored NNFN allows significantly faster optimization than NNFN, which validates the efficiency of using the factored form. Moreover, factored NNFN is also much faster than the other factored form regularizers. This is because solver

of factored nuclear norm uses the costly QR decomposition to solve the least squares subproblem, BPMF uses expensive Markov chain Monte Carlo in inference, while factored GSR involves coupled iterative algorithms. As for comparing with the other nonconvex regularizers, factored NNFN is orders of magnitude faster. Optimization with the truncated  $\ell_{1-2}$  is exceptionally slow, which is due to the need of having two levels of DCA and ADMM iterations. Figure 2 shows convergence of the testing NMSE with (training) clock time. As can be seen, factored NNFN always has the fastest convergence to the lowest NMSE.

Table 3: Performance on the synthetic data with different dimensionalities ( $m$ 's). For each data set, its sparsity ratio is shown in brackets. Error is the testing NMSE scaled by  $10^{-2}$ . The best and comparable results (according to the pairwise t-test with 95% confidence) are highlighted in bold.

	$m = 500$ (12.43%)		$m = 1000$ (6.91%)		$m = 2000$ (3.80%)	
	error	time (s)	error	time (s)	error	time (s)
nuclear	4.36	2.1	3.75	4.2	3.33	40.9
factored nuclear	2.46	0.08	2.18	0.3	1.98	1.5
BPMF	2.34	3.2	2.03	5.8	1.88	48.3
factored GSR	2.19	0.5	1.97	4.2	1.85	6.7
truncated $\ell_{1-2}$	<b>1.96</b>	695.8	<b>1.82</b>	1083.2	<b>1.77</b>	3954.1
capped- $\ell_1$	<b>1.97</b>	0.8	<b>1.83</b>	5.4	<b>1.78</b>	36.0
LSP	<b>1.97</b>	0.8	<b>1.83</b>	5.1	<b>1.77</b>	35.1
MCP	<b>1.96</b>	0.7	<b>1.82</b>	4.1	<b>1.78</b>	40.6
NNFN	<b>1.96</b>	2.1	<b>1.82</b>	7.7	<b>1.77</b>	43.1
factored NNFN	<b>1.96</b>	<b>0.04</b>	<b>1.82</b>	<b>0.08</b>	<b>1.77</b>	<b>0.3</b>

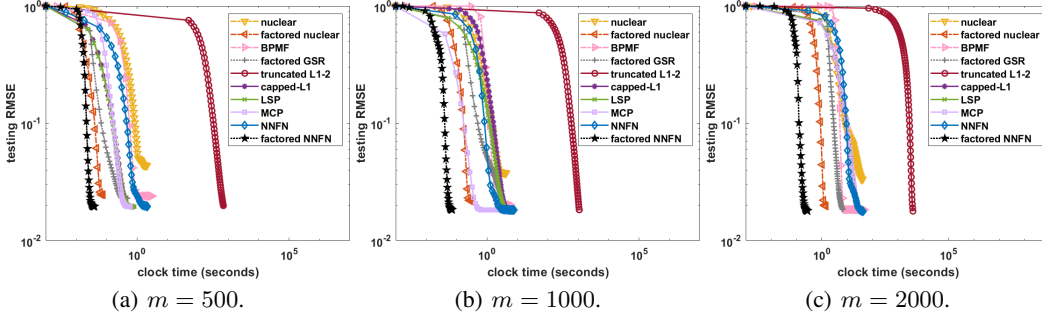


Figure 2: Testing NMSE versus clock time on the synthetic data sets.

#### 4.2.2 Effects of Noise, Rank and Sparsity Ratio

In this section, we vary (i) the variance of the Gaussian noise matrix  $\mathbf{E}$  in the range  $\{0.01, 0.1, 1\}$ ; (ii) the true rank  $k^*$  of the data in  $\{5, 10, 20\}$ ; and (iii) the sparsity ratio  $s$  in  $\{0.5, 1, 2\} \times (2mk^* \log(m)/m^2)$ . The experiment is performed on the synthetic data set, with  $m = 1000$ . In each trial, we only vary one variable while keeping the others at default ( $k^* = 5$ ,  $\mathbf{E} \sim \mathcal{N}(0, 0.1)$  and  $s = 6.91\%$ ). Figure 3 shows the testing NMSE results. As expected, a larger noise<sup>2</sup>, smaller true rank, or sparser matrix lead to a harder matrix completion problem and subsequently higher NMSE's. However, the relative performance ranking of the various methods remain the same, and nonconvex regularization always obtain the best NMSE. Different settings do not affect the relative time results (results are in Appendix B.2). factored NNFN is consistently faster than the others.

<sup>2</sup>Please note that the Y axes have different limits in Figure 3(a).

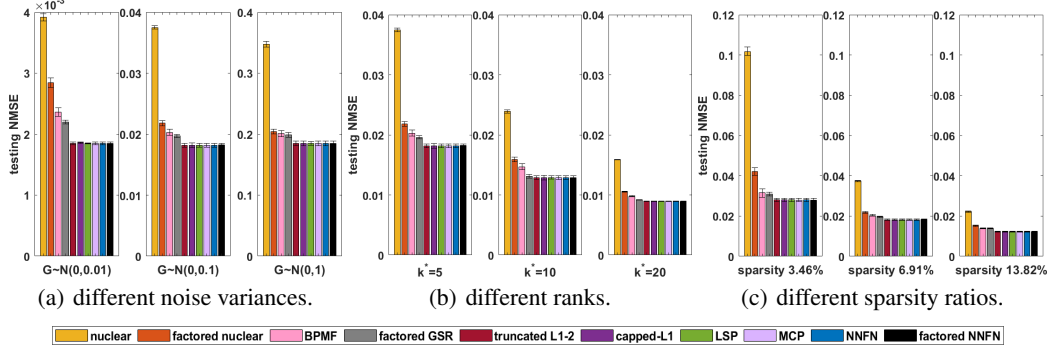


Figure 3: Testing NMSE with different settings on synthetic data ( $m = 1000$ ).

### 4.3 Real-World Data

In this section, experiments are performed on three kinds of popular benchmark data sets (details reported in Appendix B.1): (i) recommendation data [23]; (ii) hyperspectral images [39]; and (iii) climate data [1].

#### 4.3.1 Recommendation Data

The popular *MovieLens-1M* data set [18] (of size  $6,040 \times 3,449$ ), *MovieLens-10M* data set [18] (of size  $69,878 \times 10,677$ ) and *Yahoo* [23] data set (of size  $249,012 \times 296,111$ ) are used. We uniformly sample 50% of the ratings as observed for training, 25% for validation (hyperparameter tuning) and the rest for testing. Figure 4 shows convergence of the testing RMSE. Again, factored NNFN converges much faster than the other methods to a lower testing RMSE (which is consistent with recovery performance and timing results reported in Appendix B.2). Optimization with the nuclear norm, truncated  $\ell_{1-2}$  and NNFN cannot converge in three hours on *MovieLens-10M* and *Yahoo*, and thus are not reported. Factored GSR runs out of memory on *MovieLens-10M* and *Yahoo* as it requires full matrices.

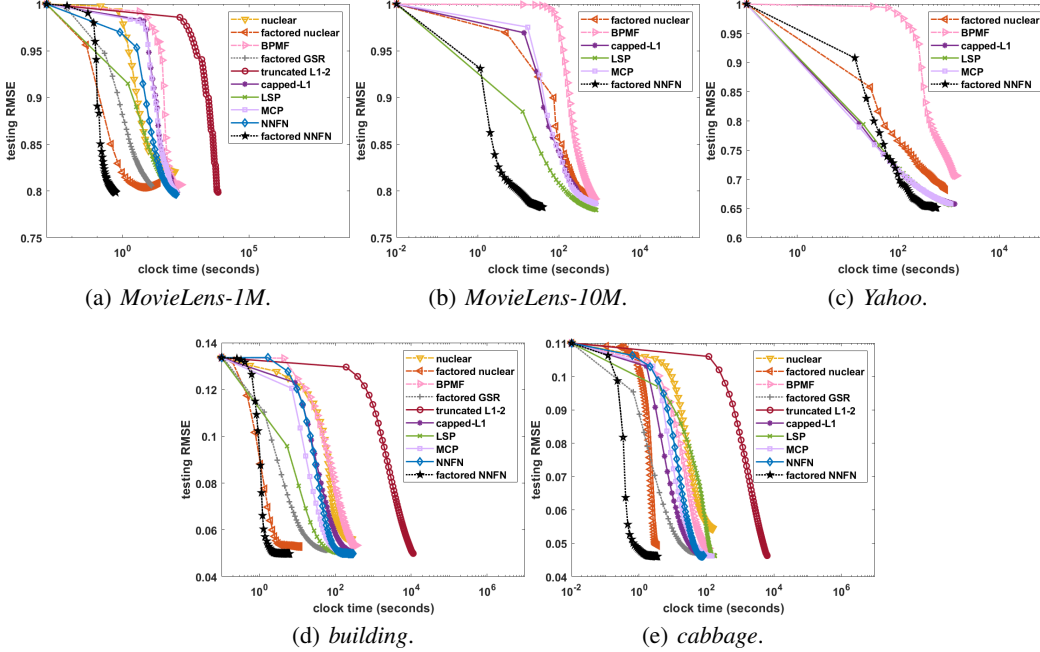


Figure 4: Testing RMSE versus clock time on the recommendation (first row) and hyperspectral (second row) data.

### 4.3.2 Hyperspectral Data

Hyperspectral images of *building* and *cabbage* from [39] are used. Each hyperspectral image originally has resolution  $I_1 \times I_2$  and  $I_3$  spectral bands, and is converted to a  $I_1 I_2 \times I_3$  matrix. The resultant *building* is of size  $1258208 \times 49$  and *cabbage* is of size  $692736 \times 49$ . The task is to fill in the missing pixels. The pixels are normalized to zero mean and unit variance, and noise from  $\mathcal{N}(0, 0.01)$  added. We randomly sample 5% of the pixels for training, 5% for validation and the rest for testing. Figure 4 shows convergence of the testing RMSE. As can be seen, nonconvex regularizers obtain the best recovery performance than the other methods. In terms of speed, factored NNFN is again the fastest. Similar observations on recovery error and timing results (reported in Appendix B.2) show that only factored NNFN is both efficient and effective.

### 4.3.3 Climate Data

The *GAS* and *USHCN* data sets from [1] are used. *GAS* contains monthly observations for the green gas components, of which we use  $CO_2$  and  $H_2$ . *USHCN* contains monthly temperature and precipitation readings. For these two data sets, some rows (which correspond to locations) of the observed matrix are completely missing. The task is to predict climate observations for locations that do not have any records. Following [1], we normalize the data to zero mean and unit variance, then randomly sample 10% of the locations for training, another 10% for validation, and the rest for testing. To allow generalization to these completely unknown locations, we follow [1] and add a graph Laplacian regularizer to (1). Specifically, the  $m$  locations are represented as nodes on a graph. The affinity matrix  $\mathbf{A} = [A_{ij}] \in \mathbb{R}^{m \times m}$ , which contains pairwise node similarities, is computed as  $A_{ij} = \exp(-2b(i, j))$ , where  $b(i, j)$  is the Haversine distance between locations  $i$  and  $j$ . The graph Laplacian regularizer is then defined as  $a(\mathbf{X}) = \text{tr}(\mathbf{X}^\top (\mathbf{D} - \mathbf{A}) \mathbf{X})$ , where  $D_{ii} = \sum_j A_{ij}$ . For the factored models (factored nuclear norm, BPMF and factored NNFN), we write  $a(\mathbf{X})$  as  $a(\mathbf{W}\mathbf{H}^\top)$ . Additionally, we compare with graph regularized alternating least squares (GRALS) [31], which optimizes for factored nuclear norm with  $a(\mathbf{W})$ .

Table 4: Performance on the climate data sets. Error is RMSE scaled by  $10^{-1}$ . The best and comparable results (according to the pairwise t-test with 95% confidence) are highlighted in bold.

	<i>GAS</i>				<i>USHCN</i>			
	$CO_2$		$H_2$		<i>temperature</i>		<i>precipitation</i>	
	error	time(s)	error	time(s)	error	time(s)	error	time(s)
nuclear	5.84	1.0	5.93	0.8	4.80	108.5	8.28	84.9
factored nuclear	5.65	0.17	5.74	0.19	4.83	15.7	8.23	33.3
BPMF	5.52	3.2	5.54	3.4	4.64	148.1	8.19	125.1
GRALS	5.65	0.7	5.78	0.4	4.98	37.2	8.18	49.6
truncated $\ell_{1-2}$	<b>5.30</b>	11.0	<b>5.31</b>	7.3	<b>4.44</b>	573.9	<b>8.06</b>	318.5
capped- $\ell_1$	5.33	0.6	<b>5.31</b>	0.7	4.50	108.5	<b>8.06</b>	87.2
LSP	5.37	1.2	5.40	1.3	4.48	133.3	<b>8.06</b>	105.8
MCP	<b>5.30</b>	1.0	5.34	0.5	<b>4.44</b>	92.5	<b>8.06</b>	85.2
NNFN	<b>5.30</b>	0.4	<b>5.31</b>	0.5	<b>4.44</b>	57.1	<b>8.06</b>	66.4
factored NNFN	<b>5.30</b>	<b>0.05</b>	<b>5.31</b>	<b>0.05</b>	<b>4.44</b>	<b>5.9</b>	<b>8.06</b>	<b>13.5</b>

Results are shown in Table 4. They are consistent with the observations in the previous experiments. In terms of recovery performance, all the nonconvex regularizers (including NNFN and factored NNFN) have comparable performance and obtain the lowest testing RMSE. In terms of speed, factored NNFN is again the fastest, and its speed advantage is particularly apparent on the larger *USHCN* data set. Figure 5 shows the convergence of RMSE on data sets that are removed from the main text due to space limitation. As shown, nonconvex regularizers generally obtain better testing RMSEs. Among them, factored NNFN is the fastest in convergence. This again validates the efficiency and effectiveness of factored NNFN.

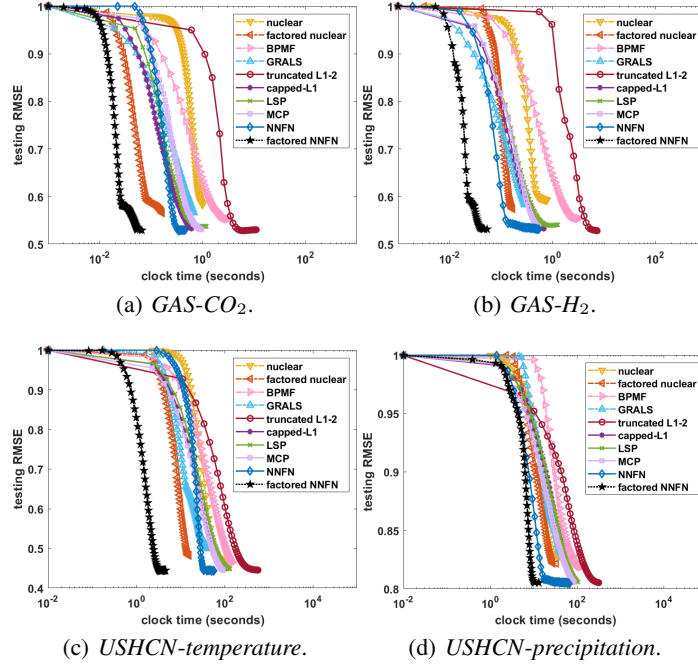


Figure 5: Testing RMSE versus clock time on climate data.

## 5 Conclusion

We propose a scalable adaptive nonconvex regularizer for low-rank matrix learning. Unlike existing adaptive nonconvex regularizers, this regularizer can be formulated into a factored matrix form which bypasses the computation of the expensive SVD. We show that learning with this factored form guarantees stable recovery and can be optimized by general solvers such as gradient-based method with convergence guarantee. Extensive experiments show that the proposed algorithm achieves state-of-the-art recovery performance comparable with the existing regularizers, but is consistently much more efficient than existing low-rank convex / nonconvex regularization and factored regularization methods.

## References

- [1] M. T. Bahadori, Q. R. Yu, and Y. Liu. Fast multivariate spatio-temporal analysis via low rank tensor learning. In *Advances in Neural Information Processing Systems*, pages 3491–3499, 2014.
- [2] N. Boumal and P.-A. Absil. Low-rank matrix completion via preconditioned optimization on the grassmann manifold. *Linear Algebra and its Applications*, 475:200–239, 2015.
- [3] S. Boyd, N. Parikh, E. Chu, B. Peleato, and J. Eckstein. Distributed optimization and statistical learning via the alternating direction method of multipliers. *Foundations and Trends in Machine Learning*, 3(1):1–122, 2011.
- [4] S. P. Boyd and L. Vandenberghe. *Convex Optimization*. Cambridge University Press, 2004.
- [5] J.-F. Cai, E. J. Candès, and Z. Shen. A singular value thresholding algorithm for matrix completion. *SIAM Journal on Optimization*, 20(4):1956–1982, 2010.
- [6] E. J. Candès, X. Li, Y. Ma, and J. Wright. Robust principal component analysis? *Journal of the ACM*, 58(3):1–37, 2011.
- [7] E. J. Candès and B. Recht. Exact matrix completion via convex optimization. *Foundations of Computational Mathematics*, 9(6):717–772, 2009.
- [8] E. J. Candès and T. Tao. Decoding by linear programming. *IEEE Transactions on Information Theory*, 51(12):4203–4215, 2005.

- [9] E. J. Candes, M. B. Wakin, and S. P. Boyd. Enhancing sparsity by reweighted  $\ell_1$  minimization. *Journal of Fourier Analysis and Applications*, 14(5-6):877–905, 2008.
- [10] J. Chen, J. Zhou, and J. Ye. Integrating low-rank and group-sparse structures for robust multi-task learning. In *International Conference on Knowledge Discovery and Data Mining*, pages 42–50, 2011.
- [11] D. L. Donoho, I. M. Johnstone, G. Kerkyacharian, and D. Picard. Wavelet shrinkage: Asymptopia? *Journal of the Royal Statistical Society: Series B*, 57(2):301–337, 1995.
- [12] J. Fan, L. Ding, Y. Chen, and M. Udell. Factor group-sparse regularization for efficient low-rank matrix recovery. In *Advances in Neural Information Processing Systems*, pages 5104–5114, 2019.
- [13] M. Fazel. *Matrix Rank Minimization with Applications*. PhD thesis, Stanford, 2002.
- [14] W. R. Gilks, S. Richardson, and D. Spiegelhalter. *Markov Chain Monte Carlo in Practice*. CRC Press, 1995.
- [15] S. Gu, L. Zhang, W. Zuo, and X. Feng. Weighted nuclear norm minimization with application to image denoising. In *Conference on Computer Vision and Pattern Recognition*, pages 2862–2869, 2014.
- [16] H. Gui, J. Han, and Q. Gu. Towards faster rates and oracle property for low-rank matrix estimation. In *International Conference on Machine Learning*, pages 2300–2309, 2016.
- [17] S. Gunasekar, B. E. Woodworth, S. Bhojanapalli, B. Neyshabur, and N. Srebro. Implicit regularization in matrix factorization. In *Advances in Neural Information Processing Systems*, pages 6151–6159, 2017.
- [18] F. M. Harper and J. A. Konstan. The movielens datasets: History and context. *ACM Transactions on Interactive Intelligent Systems*, 5(4):1–19, 2015.
- [19] T. Hastie, R. Mazumder, J. D. Lee, and R. Zadeh. Matrix completion and low-rank svd via fast alternating least squares. *Journal of Machine Learning Research*, 16(1):3367–3402, 2015.
- [20] J.-B. Hiriart-Urruty. Generalized differentiability, duality and optimization for problems dealing with differences of convex functions. In *Proceedings of the Symposium on Convexity and Duality in Optimization*, pages 37–70, 1985.
- [21] Y. Hu, D. Zhang, J. Ye, X. Li, and X. He. Fast and accurate matrix completion via truncated nuclear norm regularization. *IEEE Transactions on Pattern Analysis and Machine Intelligence*, 35(9):2117–2130, 2012.
- [22] A. Jennings and J. McKeown. *Matrix Computation*. John Wiley & Sons, 1992.
- [23] Y. Koren, R. Bell, and C. Volinsky. Matrix factorization techniques for recommender systems. *Computer*, 42(8):30–37, 2009.
- [24] G. Liu, Z. Lin, S. Yan, J. Sun, Y. Yu, and Y. Ma. Robust recovery of subspace structures by low-rank representation. *IEEE Transactions on Pattern Analysis and Machine Intelligence*, 35(1):171–184, 2012.
- [25] C. Lu, C. Zhu, C. Xu, S. Yan, and Z. Lin. Generalized singular value thresholding. In *AAAI Conference on Artificial Intelligence*, pages 1805–1811, 2015.
- [26] T.-H. Ma, Y. Lou, and T.-Z. Huang. Truncated  $\ell_{1-2}$  models for sparse recovery and rank minimization. *SIAM Journal on Imaging Sciences*, 10(3):1346–1380, 2017.
- [27] A. Mnih and R. R. S. Probabilistic matrix factorization. In *Advances in Neural Information Processing Systems*, pages 1257–1264, 2008.
- [28] F. Nie, H. Huang, and C. Ding. Low-rank matrix recovery via efficient Schatten  $p$ -norm minimization. In *AAAI Conference on Artificial Intelligence*, 2012.
- [29] J. Nocedal and S. Wright. *Numerical Optimization*. Springer Science & Business Media, 2006.
- [30] N. Parikh and S. Boyd. Proximal algorithms. *Foundations and Trends in Optimization*, 1(3):127–239, 2014.
- [31] N. Rao, H.-F. Yu, P. K. Ravikumar, and I. S. Dhillon. Collaborative filtering with graph information: Consistency and scalable methods. In *Advances in Neural Information Processing Systems*, pages 2107–2115, 2015.

- [32] R. Salakhutdinov and A. Mnih. Bayesian probabilistic matrix factorization using markov chain monte carlo. In *International Conference on Machine Learning*, pages 880–887, 2008.
- [33] F. Shang, Y. Liu, and J. Cheng. Tractable and scalable Schatten quasi-norm approximations for rank minimization. In *Artificial Intelligence and Statistics*, pages 620–629, 2016.
- [34] N. Srebro, J. Rennie, and T. S. Jaakkola. Maximum-margin matrix factorization. In *Advances in Neural Information Processing Systems*, pages 1329–1336, 2005.
- [35] S. Tu, R. Boczar, M. Simchowitz, M. Soltanolkotabi, and B. Recht. Low-rank solutions of linear matrix equations via Procrustes flow. In *International Conference on Machine Learning*, pages 964–973, 2016.
- [36] B. Vandereycken. Low-rank matrix completion by Riemannian optimization. *SIAM Journal on Optimization*, 23(2):1214–1236, 2013.
- [37] L. Wang, X. Zhang, and Q. Gu. A unified computational and statistical framework for nonconvex low-rank matrix estimation. In *Artificial Intelligence and Statistics*, pages 981–990, 2017.
- [38] Z. Wen, W. Yin, and Y. Zhang. Solving a low-rank factorization model for matrix completion by a nonlinear successive over-relaxation algorithm. *Mathematical Programming Computation*, 4(4):333–361, 2012.
- [39] Q. Yao, J. T. Kwok, T. Wang, and T.-Y. Liu. Large-scale low-rank matrix learning with nonconvex regularizers. *IEEE Transactions on Pattern Analysis and Machine Intelligence*, 41(11):2628–2643, 2019.
- [40] C.-H. Zhang. Nearly unbiased variable selection under minimax concave penalty. *The Annals of Statistics*, 38(2):894–942, 2010.
- [41] T. Zhang. Analysis of multi-stage convex relaxation for sparse regularization. *Journal of Machine Learning Research*, 11(Mar):1081–1107, 2010.

## A Proof

### A.1 Proposition 3.1

*Proof.* Let  $\mathbf{X} = \mathbf{U}\text{Diag}(\tilde{\boldsymbol{\sigma}})\mathbf{V}^\top$  and  $\mathbf{Z} = \bar{\mathbf{U}}\text{Diag}(\boldsymbol{\sigma}(\mathbf{Z}))\bar{\mathbf{V}}^\top$  be the SVD decomposition of  $\mathbf{X}$  and  $\mathbf{Z}$ . By simple expansion, we have

$$\begin{aligned} & \frac{1}{2}\|\mathbf{X} - \mathbf{Z}\|_F^2 + \lambda r_{\text{NNFN}}(\mathbf{X}) \\ &= \frac{1}{2}\text{tr}(\mathbf{X}^\top \mathbf{X} + \mathbf{Z}^\top \mathbf{Z} - 2\mathbf{X}^\top \mathbf{Z}) + \lambda(\|\mathbf{X}\|_* - \theta\|\mathbf{X}\|_F) \\ &= \frac{1}{2}(\|\tilde{\boldsymbol{\sigma}}\|_2^2 + \|\boldsymbol{\sigma}(\mathbf{Z})\|_2^2) - \text{tr}(\mathbf{X}^\top \mathbf{Z}) + \lambda\|\tilde{\boldsymbol{\sigma}}\|_1 - \lambda\theta\|\tilde{\boldsymbol{\sigma}}\|_2. \end{aligned}$$

Recall that  $\text{tr}(\mathbf{X}^\top \mathbf{Z}) \leq \tilde{\boldsymbol{\sigma}}^\top \boldsymbol{\sigma}(\mathbf{Z})$  achieves its equality at  $\mathbf{U} = \bar{\mathbf{U}}, \mathbf{V} = \bar{\mathbf{V}}$  [22]. Then solving (5) can be instead computed by solving  $\tilde{\boldsymbol{\sigma}}$  as

$$\begin{aligned} & \arg \min_{\tilde{\boldsymbol{\sigma}}} \frac{1}{2}\|\tilde{\boldsymbol{\sigma}} - \boldsymbol{\sigma}(\mathbf{Z})\|_2^2 + \lambda(\|\tilde{\boldsymbol{\sigma}}\|_1 - \theta\|\tilde{\boldsymbol{\sigma}}\|_2) \\ & \text{s.t. } \tilde{\sigma}_1 \geq \tilde{\sigma}_2 \geq \dots \geq \tilde{\sigma}_m \geq 0. \end{aligned} \quad (8)$$

It can be solved by proximal operator as  $\tilde{\boldsymbol{\sigma}} = \text{prox}_{\lambda\|\cdot\|_{1-2}}(\boldsymbol{\sigma}(\mathbf{Z}))$ . The constraint in (8) is naturally satisfied. As  $\sigma_i(\mathbf{Z}) \geq 0$  and  $\sigma_i(\mathbf{Z}) \geq \sigma_{i+1}(\mathbf{Z}) \forall i$ , we must have  $\tilde{\sigma}_i \geq 0$  and  $\tilde{\sigma}_i \geq \tilde{\sigma}_{i+1} \forall i$ . Otherwise, we can always swap the sign or value of  $\tilde{\sigma}_i$  and  $\tilde{\sigma}_{i+1}$  and obtain a smaller objective of (8).  $\square$

### A.2 Proposition 3.2

*Proof.* Let  $\mathbf{X} = \mathbf{U}\text{Diag}(\tilde{\boldsymbol{\sigma}})\mathbf{V}^\top$  where  $\tilde{\boldsymbol{\sigma}} = \text{prox}_{\lambda\|\cdot\|_{1-2}}(\boldsymbol{\sigma}(\mathbf{Z}))$ . Now we prove that

- shrinkage:  $\sigma_i(\mathbf{Z}) \geq \tilde{\sigma}_i$ ,
- adaptivity:  $\sigma_i(\mathbf{Z}) - \tilde{\sigma}_i \leq \sigma_{i+1}(\mathbf{Z}) - \tilde{\sigma}_{i+1}$ , where the strict inequality holds at least for one  $i$ .

The first point: From Proposition 3.1, we can see the optimization problem on matrix (5) can be transformed to an optimization problem on singular values (8). As shown in Proposition 3.1, for  $\tilde{\boldsymbol{\sigma}} = \text{prox}_{\lambda\|\cdot\|_{1-2}}(\boldsymbol{\sigma}(\mathbf{Z}))$ , we have  $\sigma_i(\mathbf{Z}) \geq \tilde{\sigma}_i \geq 0$ .

The second point: The optimal of (8) satisfies

$$\tilde{\boldsymbol{\sigma}} - \boldsymbol{\sigma}(\mathbf{Z}) + \lambda - \lambda \frac{\tilde{\boldsymbol{\sigma}}}{\|\tilde{\boldsymbol{\sigma}}\|_2} = 0.$$

As  $\sigma_i(\mathbf{Z}) \geq \tilde{\sigma}_i \geq 0$ , we have

$$\sigma_i(\mathbf{Z}) - \tilde{\sigma}_i = \lambda - \lambda \frac{\tilde{\sigma}_i}{\|\tilde{\boldsymbol{\sigma}}\|_2} \geq 0.$$

Then as  $\tilde{\sigma}_i \geq \tilde{\sigma}_{i+1}$ , we have

$$\lambda - \lambda \frac{\tilde{\sigma}_i}{\|\tilde{\boldsymbol{\sigma}}\|_2} \leq \lambda - \lambda \frac{\tilde{\sigma}_{i+1}}{\|\tilde{\boldsymbol{\sigma}}\|_2},$$

and correspondingly  $\sigma_i(\mathbf{Z}) - \tilde{\sigma}_i \leq \sigma_{i+1}(\mathbf{Z}) - \tilde{\sigma}_{i+1}$ . The inequality holds only when  $\sigma_i(\mathbf{Z}) \neq \sigma_{i+1}(\mathbf{Z})$ .  $\square$

### A.3 Corollary 3.3

**Lemma A.1.** Let  $\hat{r}(\alpha)$  be a nonlinear, concave and non-decreasing function for  $\alpha \geq 0$  with  $\hat{r}(0) = 0$ , and

$$p = \arg \min_x \frac{1}{2}(x - z)^2 + \lambda \hat{r}(|x|). \quad (9)$$

Then, when  $z \geq 0$ , we have

- $0 \leq p \leq z$ ,
- $z_1 - p(z_1) \leq z_2 - p_2$  for  $z_1 \geq z_2$ .

*Proof.* The first point: Obvious, when  $z \geq 0, p \geq 0$ . Next, we prove  $p \leq z$  by contradiction. Assume that  $p > z$ . Then as  $\hat{r}$  is non-decreasing, we have

$$\hat{r}(|p|) \geq \hat{r}(|z|).$$

Therefore we get

$$\frac{1}{2}(p - z)^2 + \lambda \hat{r}(|z'|) > \frac{1}{2}(z - z)^2 + \lambda \hat{r}(|z|),$$

which leads to a contradiction that  $p$  is the minimum solution found by optimizing (9). Thus,  $p \leq z$ .

The second point: The optimal of (9)  $p$  satisfies

$$p - z + \lambda \partial \hat{r}(p) = 0. \quad (10)$$

As  $\hat{r}$  is concave, for  $z_1 \geq z_2$ , we have

$$\partial \hat{r}(p_1) \leq \partial \hat{r}(p_2). \quad (11)$$

Combining (11) and (10), we get

$$z_1 - p_1 \leq z_2 - p_2,$$

and the second point is proved.  $\square$

Now, we can prove Proposition 3.2.

*Proof.* As introduced in Section 2, common nonconvex regularizers (Table 5) can be written into (3).

Table 5: Common nonconvex low-rank regularizers.

	$\hat{r}(\sigma_i(\mathbf{X}))$
capped- $\ell_1$ [41]	$\min(\sigma_i(\mathbf{X}), \theta)$
LSP [9]	$\log\left(\frac{1}{\theta}\sigma_i(\mathbf{X}) + 1\right)$
MCP [40]	$\begin{cases} \sigma_i(\mathbf{X}) - \frac{\sigma_i^2(\mathbf{X})}{2\theta\lambda} & \text{if } \sigma_i(\mathbf{X}) \leq \theta\lambda \\ \frac{\theta\lambda}{2} & \text{otherwise} \end{cases}$

Let the SVD of  $\mathbf{Z}$  be  $\bar{\mathbf{U}}\text{Diag}(\boldsymbol{\sigma}(\mathbf{Z}))\bar{\mathbf{V}}^\top$ . From Theorem 1 in [25], we have

$$\bar{\mathbf{X}} \equiv \text{prox}_{\lambda\hat{r}}(\mathbf{Z}) = \bar{\mathbf{U}}\text{Diag}(\tilde{\boldsymbol{\sigma}})\bar{\mathbf{V}}^\top,$$

where  $\tilde{\sigma}_i = \text{prox}_{\lambda\hat{r}}(\sigma_i(\mathbf{Z}))$ . Then, as every singular value  $\sigma_i(\mathbf{Z})$  is nonnegative, by Lemma A.1, we get the conclusion. Note that since  $\hat{r}$  is not linear, thus the strict inequality in  $\sigma_i(\mathbf{Z}) - \tilde{\sigma}_i \leq \sigma_{i+1}(\mathbf{Z}) - \tilde{\sigma}_{i+1}$  holds at least for one  $i$ .  $\square$

#### A.4 Theorem 3.4

*Proof.* Consider  $f(\mathbf{X}) = \frac{1}{2}\|\mathcal{A}(\mathbf{X}) - \mathbf{b}\|_2^2$  with affine transformation  $\mathcal{A}$ . Assume the final  $\mathbf{X}^t$  satisfies

$$c_1^2\|\mathbf{e}\|^2/2 \leq f(\mathbf{X}^t) \leq (c_1^2 + \epsilon)\|\mathbf{e}\|_2^2/2, \quad (12)$$

where  $c_1 \geq 0, \epsilon \geq 0$ . Assume  $\mathbf{X}^t \leq k^*$ . Obviously, the optimal  $\mathbf{X}^*$  satisfies  $\mathbf{b} - \mathcal{A}(\mathbf{X}^*) = \mathbf{e}$  and hence  $f(\mathbf{X}^*) = \frac{1}{2}\|\mathcal{A}(\mathbf{X}^*) - \mathbf{b}\|_2^2 = \frac{\|\mathbf{e}\|_2^2}{2}$ .

We can derive

$$\begin{aligned}
\|\mathcal{A}(\mathbf{X}^* - \mathbf{X}^t)\|_2^2 &\leq \|(\mathbf{b} - \mathcal{A}(\mathbf{X}^t)) - \mathbf{e}\|_2^2, \\
&\leq 2 \left( f(\mathbf{X}^t) - \mathbf{e}^\top (\mathbf{b} - \mathcal{A}(\mathbf{X}^t)) + \frac{\|\mathbf{e}\|_2^2}{2} \right), \\
&\leq 2 \left( f(\mathbf{X}^t) + \frac{2}{c_1} f(\mathbf{X}^t) + \frac{1}{c_1^2} f(\mathbf{X}^t) \right), \\
&\leq 2 \left( 1 + \frac{1}{c_1} \right)^2 f(\mathbf{X}^t)
\end{aligned} \tag{13}$$

Now, we are ready to bound the difference between  $\mathbf{X}^t$  and the optimal  $\mathbf{X}^*$ .

$$\|\mathbf{X}^t - \mathbf{X}^*\|_F^2 \leq \frac{1}{1 - \delta_{2k^*}} \|\mathcal{A}(\mathbf{X}^t - \mathbf{X}^*)\|_2^2 \tag{14}$$

$$\leq \frac{2}{1 - \delta_{2k^*}} \left( 1 + \frac{1}{c_1} \right)^2 f(\mathbf{X}^t) \tag{15}$$

$$\begin{aligned}
&\leq \frac{1}{1 - \delta_{2k^*}} \left( 1 + \frac{1}{c_1} \right)^2 (c_1^2 + \epsilon) \|\mathbf{e}\|_2^2 \\
&= \frac{(c_1 + 1)^2 (c_1^2 + \epsilon) \|\mathbf{e}\|_2^2}{c_1^2 (1 - \delta_{2k^*})},
\end{aligned} \tag{16}$$

where (14) is derived from RIP (6), and the isometry constant is  $\delta_{2k^*}$  as  $\mathbf{X}^t - \mathbf{X}^*$  is a matrix of rank at most  $2k^*$ . Then (15) is obtained using (13) and (16) is obtained using (12).

□

### A.5 Theorem 3.5

*Proof.* In (7), a regularized low-rank matrix learning problem is solved. This can be transformed into the following constrained problem [4, 29]:

$$\min_{\mathbf{W}, \mathbf{H}} f(\mathbf{W}\mathbf{H}^\top) \text{ s.t. } (\mathbf{W}, \mathbf{H}) \in \mathcal{C} \equiv \{(\mathbf{W}, \mathbf{H}) : \frac{1}{2}(\|\mathbf{W}\|_F^2 + \|\mathbf{H}\|_F^2) - \|\mathbf{W}\mathbf{H}^\top\|_F \leq \beta'\}, \tag{17}$$

where  $\beta' \geq 0$  is a hyperparameter. These two forms obtain equivalent solutions [4]. Therefore, we prove for the constrained problem, while the conclusion applies for both forms.

Let  $\mathbf{X}^t = \mathbf{W}^t(\mathbf{H}^t)^\top$  and assume that the sequence  $\{\mathbf{X}^t\}$  satisfying  $f(\mathbf{X}^{t+1}) \leq f(\mathbf{X}^t)$ . This sequence can be obtained by optimizing (17) via projected gradient descent which guarantees sufficient decrease in  $f$  [4, 29].

Obviously, the optimal  $\mathbf{X}^*$  satisfies  $\mathbf{b} - \mathcal{A}(\mathbf{X}^*) = \mathbf{e}$  and hence  $f(\mathbf{X}^*) = \frac{1}{2} \|\mathcal{A}(\mathbf{X}^*) - \mathbf{b}\|_2^2 = \frac{\|\mathbf{e}\|_2^2}{2}$ . Thus  $\mathbf{X}^t$  obtained at the  $t$ th iteration satisfies  $f(\mathbf{X}^t) \geq \frac{c_1^2 \|\mathbf{e}\|_2^2}{2} \geq \frac{\|\mathbf{e}\|_2^2}{2}$  for constant  $c_1$  whose absolute value is larger than 1. By choosing the dimension  $k$  of  $\mathbf{W} \in \mathbb{R}^{m \times k}$ , one can let  $\mathbf{X}^t \leq k^*$ , where  $k^*$  is the true rank of the optimal matrix  $\mathbf{X}^*$ .

We can derive

$$\begin{aligned}
\|\mathcal{A}(\mathbf{X}^* - \mathbf{X}^t)\|_2^2 &\leq \|(\mathbf{b} - \mathcal{A}(\mathbf{X}^t)) - \mathbf{e}\|_2^2, \\
&\leq 2 \left( f(\mathbf{X}^t) - \mathbf{e}^\top (\mathbf{b} - \mathcal{A}(\mathbf{X}^t)) + \frac{\|\mathbf{e}\|_2^2}{2} \right), \\
&\leq 2 \left( f(\mathbf{X}^t) + \frac{2}{c_1} f(\mathbf{X}^t) + \frac{1}{c_1^2} f(\mathbf{X}^t) \right), \\
&\leq 2 \left( 1 + \frac{1}{c_1} \right)^2 f(\mathbf{X}^t)
\end{aligned} \tag{18}$$

Now, we are ready to bound the difference between this  $\mathbf{X}^t$  and the optimal  $\mathbf{X}^*$ .

$$\|\mathbf{X}^t - \mathbf{X}^*\|_F^2 \leq \frac{1}{1 - \delta_{2k^*}} \|\mathcal{A}(\mathbf{X}^t - \mathbf{X}^*)\|_2^2 \quad (19)$$

$$\leq \frac{2}{1 - \delta_{2k^*}} \left(1 + \frac{1}{c_1}\right)^2 f(\mathbf{X}^t) \quad (20)$$

$$\begin{aligned} &\leq \frac{1}{1 - \delta_{2k^*}} \left(1 + \frac{1}{c_1}\right)^2 (c_1^2 + \epsilon) \|\mathbf{e}\|_2^2 \\ &= \frac{(c_1 + 1)^2 (c_1^2 + \epsilon) \|\mathbf{e}\|_2^2}{c_1^2 (1 - \delta_{2k^*})}, \end{aligned} \quad (21)$$

where the isometry constant is  $\delta_{2k^*}$  as  $\mathbf{X}^t - \mathbf{X}^*$  is a matrix of rank at most  $2k^*$ , (19) is derived from RIP, (20) comes from (18), and (21) is obtained as one can choose a small constant  $\epsilon$  such that  $\frac{(c_1^2 + \epsilon) \|\mathbf{e}\|_2^2}{2} \geq f(\mathbf{X}^t) \geq \frac{c_1^2 \|\mathbf{e}\|_2^2}{2}$ .

□

### A.6 Theorem 3.6

*Proof.* For smooth functions, gradient descent can obtain sufficient decrease as shown in the following Proposition.

**Proposition A.2** ([29]). *A differentiable function  $h$  with  $L$ -Lipschitz continuous gradient, i.e.,  $\|\nabla_x h(x^t) - \nabla_x h(x^{t+1})\|_2 \leq L\|x^t - x^{t+1}\|_2$ , satisfies the following inequality,*

$$h(x^t) - h(x^{t+1}) \geq \frac{1}{2L} \|\nabla_x h(x^t)\|_2^2.$$

Moreover, when  $h$  is bounded from below, i.e.,  $\inf h(x) > -\infty$  and  $\lim_{\|x\|_2 \rightarrow \infty} h(x) = \infty$ , optimizing  $h$  by gradient descent is guaranteed to converge.

Since  $\mathbf{W}_t \mathbf{H}_t^\top \neq \mathbf{0}$ ,  $F(\mathbf{W}, \mathbf{H})$  is smooth. As gradient descent is used, we then have

$$F(\mathbf{W}^t, \mathbf{H}^t) - F(\mathbf{W}^{t+1}, \mathbf{H}^{t+1}) \geq \frac{\eta}{2} \|\nabla_{\mathbf{W}} F(\mathbf{W}^t, \mathbf{H}^t)\|_F^2 + \frac{\eta}{2} \|\nabla_{\mathbf{H}} F(\mathbf{W}^t, \mathbf{H}^t)\|_F^2.$$

At the  $(T+1)$ th iteration, the difference between  $F(\mathbf{W}^1, \mathbf{H}^1)$  and  $F(\mathbf{W}^{T+1}, \mathbf{H}^{T+1})$  is calculated as

$$F(\mathbf{W}^1, \mathbf{H}^1) - F(\mathbf{W}^{T+1}, \mathbf{H}^{T+1}) \geq \sum_{t=1}^T \frac{\eta}{2} \|\nabla_{\mathbf{W}} F(\mathbf{W}^t, \mathbf{H}^t)\|_F^2 + \frac{\eta}{2} \|\nabla_{\mathbf{H}} F(\mathbf{W}^t, \mathbf{H}^t)\|_F^2. \quad (22)$$

As assumed,  $\lim_{\|\mathbf{W}\|_F \rightarrow \infty} F(\mathbf{W}, \cdot) = \infty$ ,  $\lim_{\|\mathbf{H}\|_F \rightarrow \infty} F(\cdot, \mathbf{H}) = \infty$ . Thus  $\infty > F(\mathbf{W}^1, \mathbf{H}^1) - F(\mathbf{W}^{T+1}, \mathbf{H}^{T+1}) \geq c$ , where  $c$  is a finite constant. Combining this with (22), when  $T \rightarrow \infty$ , we see that a sum of infinite sequence is smaller than a finite constant. This means the sequence  $\{\mathbf{W}^t, \mathbf{H}^t\}$  has limit points. Let  $\{\bar{\mathbf{W}}, \bar{\mathbf{H}}\}$  be a limit point, we must have

$$\nabla_{\mathbf{W}} F(\bar{\mathbf{W}}, \bar{\mathbf{H}}) = \mathbf{0} \text{ and } \nabla_{\mathbf{H}} F(\bar{\mathbf{W}}, \bar{\mathbf{H}}) = \mathbf{0}.$$

By definition, this shows  $\{\bar{\mathbf{W}}, \bar{\mathbf{H}}\}$  is a critical point of (7).

Next, we proceed to prove that  $\bar{\mathbf{X}} = \bar{\mathbf{W}} \bar{\mathbf{H}}^\top$  is the the critical point of (1) with  $r(\mathbf{X}) = r_{\text{NNFN}}(\mathbf{X})$ .

As shown in [34], the nuclear norm can be reformulated in terms of factorized matrices. Then we have

$$\begin{aligned} &\min_{\mathbf{W}, \mathbf{H}} f(\mathbf{W} \mathbf{H}^\top) - \lambda \|\mathbf{W} \mathbf{H}^\top\|_F + \lambda/2 (\|\mathbf{W}\|_F^2 + \|\mathbf{H}\|_F^2) \\ &\geq \min_{\mathbf{X}} f(\mathbf{X}) - \lambda \|\mathbf{X}\|_F + \min_{\mathbf{W}, \mathbf{H}} \lambda/2 (\|\mathbf{W}\|_F^2 + \|\mathbf{H}\|_F^2) \quad \text{s.t. } \mathbf{X} = \mathbf{W} \mathbf{H}^\top \\ &\geq \min_{\mathbf{X}} f(\mathbf{X}) - \lambda \|\mathbf{X}\|_F + \lambda \|\mathbf{X}\|_*. \end{aligned}$$

Thus, if  $(\bar{\mathbf{W}}, \bar{\mathbf{H}})$  is a critical point of (7), then  $\bar{\mathbf{X}} = \bar{\mathbf{W}} (\bar{\mathbf{H}})^\top$  is also critical point of (1) with  $r(\mathbf{X}) = r_{\text{NNFN}}(\mathbf{X})$ . □

## B More on Experiments

Due to space limitation, we have to remove some details and results from the main text and present them here. In Section B.1, we introduce more details on setup of data and codes. Then in Section B.2, we present the full experimental results.

### B.1 Setup

#### B.1.1 Data

All the data sets we used are public downloadable: *MovieLens-1M* and *MovieLens-10M*<sup>3</sup>; *Yahoo*<sup>4</sup>; *building* and *cabbage*<sup>5</sup>; *GAS*<sup>6</sup>; and *USHCN*<sup>7</sup>.

#### B.1.2 Compared Methods

For the methods that we compare in the experiments, we use their public available codes.

The low-rank regularizers compared include: (i) convex nuclear norm regularizer  $\|\mathbf{X}\|_*$  [7] optimized by the recent softImpute algorithm via alternating least squares<sup>8</sup> [19]; (ii) truncated  $\ell_{1-2}$  regularizer [26] optimized with the difference of convex functions (DCA) algorithm with sub-problems solved by the alternating direction method of multipliers (ADMM)<sup>9</sup>; and (iii) nonconvex low-rank regularizers of the form (3), including the capped- $\ell_1$  penalty [41], log-sum penalty (LSP) [9]; and minimax concave penalty (MCP) [40], is optimized by the popularly used low-rank matrix learning solver FaNCL<sup>10</sup> [39].

The factored regularizers compared include: (i) factored nuclear norm [34] solved by low-rank matrix fitting algorithm (LMaFit)<sup>11</sup> [38], which directly solves  $\min_{\mathbf{W}, \mathbf{H}} f(\mathbf{W}\mathbf{H}^\top) + \frac{\lambda}{2}(\|\mathbf{W}\|_F^2 + \|\mathbf{H}\|_F^2)$ ; and (ii) Bayesian probabilistic matrix factorization (BPMF)<sup>12</sup> [27], which is a Bayesian model trained with Markov chain Monte Carlo [14]; and (iii) factored group-sparse regularizer (factored GSR)<sup>13</sup> [12] which approximates Schatten-p norm regularizer and is optimized by proximal alternating linearized minimization.

For hyperparameter tuning,  $\lambda$  in (1) is chosen from  $[10^{-3}, 10^2]$ ,  $r_t$  and  $k$  is a integer chosen from  $[1, \min(m, n)]$ , and stepsize is chosen from  $[10^{-5}, 1]$ . For the other baselines, we use the hyperparameter ranges as mentioned in the corresponding papers. All hyperparameters are tuned by grid search using the validation set.

### B.2 Results

#### B.2.1 Rank of the Recovered Matrix

In this section, we report the rank of the recovered matrix obtained by different methods on all the data sets used in Section 4.

Table 6 shows the rank obtained on synthetic data. As shown, all methods except the nuclear norm regularizer can recover the true rank value  $k^* = 5$ . Table 7 shows the rank obtained on real-world data. Although sometimes these regularizers choose the same rank (such as factored GSR, truncated  $\ell_{1-2}$  norm, NNFN and factored NNFN on *MovieLens-1M*), their recovery performances are different. As shown in Table 9 and Table 11 below, NNFN and factored NNFN obtain better recovery performance. This may be explained by the adaptive penalization on singular values.

<sup>3</sup><http://grouplens.org/datasets/movielens/>

<sup>4</sup><http://webscope.sandbox.yahoo.com/catalog.php?datatype=c>

<sup>5</sup><https://sites.google.com/site/hyperspectralcolorimaging/dataset/>

<sup>6</sup><https://viterbi-web.usc.edu/~liu32/data/NA-1990-2002-Monthly.csv>

<sup>7</sup><http://www.ncdc.noaa.gov/oa/climate/research/ushcn>

<sup>8</sup>[https://cran.r-project.org/src/contrib/softImpute\\_1.4.tar.gz](https://cran.r-project.org/src/contrib/softImpute_1.4.tar.gz), we rewrite it in MATLAB

<sup>9</sup><https://sites.google.com/site/louyifei/TL12-webcode.zip?attredirects=0&d=1>

<sup>10</sup><https://github.com/quanmingyao/FaNCL>

<sup>11</sup><https://www.caam.rice.edu/~optimization/L1/LMaFit/download.html>

<sup>12</sup><https://www.cs.toronto.edu/~rsalakhu/BPMF.html>

<sup>13</sup><https://github.com/udellgroup/Codes-of-FGSR-for-effecient-low-rank-matrix-recovery>

Table 6: Rank of the recovered matrix on the synthetic data.

	$m = 500$	$m = 1000$	$m = 2000$
nuclear	108	61	77
factored nuclear	5	5	5
BPMF	5	5	5
factored GSR	5	5	5
truncated $\ell_{1-2}$	5	5	5
capped- $\ell_1$	5	5	5
LSP	5	5	5
MCP	5	5	5
NNFN	5	5	5
factored NNFN	5	5	5

Table 7: Rank of the recovered matrix on the real-world data.  $M-1M$  and  $M-10M$  are short for *MovieLens-1M* and *MovieLens-10M*.

	<i>recommendation</i>			<i>hyperspectral</i>		<i>climate-GAS</i>		<i>climate-USHCN</i>	
	$M-1M$	$M-10M$	<i>Yahoo</i>	<i>building</i>	<i>cabbage</i>	$CO_2$	$H_2$	<i>temper.</i>	<i>precip.</i>
nuclear	27	-	-	49	49	8	7	35	121
factored nuclear	9	9	6	1	3	10	10	3	5
BPMF	9	9	6	1	3	10	9	3	5
factored GSR	5	-	-	1	3	9	10	3	5
truncated $\ell_{1-2}$	5	-	-	1	3	9	10	3	5
capped- $\ell_1$	8	9	8	1	3	5	10	6	10
LSP	9	9	9	1	3	4	8	5	5
MCP	7	9	7	1	3	9	3	3	5
NNFN	5	-	-	1	3	9	10	3	5
factored NNFN	5	9	6	1	3	9	10	3	5

### B.2.2 Effects of Noise, Rank and Sparsity Ratio on Synthetic Data

Corresponding to the examination on how noise, rank and sparsity ratio affect learning performance in Section 4.2, the timing results are shown in Figure 6. Although the exact timing results vary across different settings, the trend remains the same as observed in the main text. factored NNFN is consistently the fastest, and truncated  $\ell_{1-2}$  is the slowest.

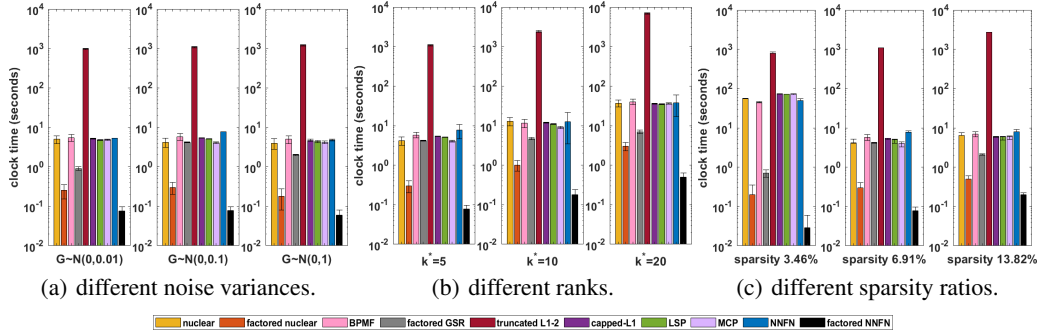


Figure 6: Clock time (seconds) obtained with different settings on the synthetic data set ( $m = 1000$ ).

### B.2.3 Full Performance Table

As mentioned in Section 4, all experimental results are averaged over five runs. In the main text, we only report the average performance due to space limitation. Here we provide results recorded as "mean  $\pm$  standard deviation" for both recovery error in terms of RMSE or NMSE and the training clock time.

Tables 8 and 11 below correspond to Tables 3 and 4 in the main text, while Table 9 and Table 10 shows the results on recommendation data and hyperspectral images. As can be seen, factored NNFN always obtains the best performance, and adaptive nonconvex regularizers are better than the other regularizers in general.

Table 8: Performance on the synthetic data with different dimensionalities ( $m$ 's). For each data set, its sparsity ratio is shown in brackets. Error is the testing NMSE scaled by  $10^{-2}$ . The best and comparable results (according to the pairwise t-test with 95% confidence) are highlighted in bold.

	$m = 500$ (12.43%)		$m = 1000$ (6.91%)		$m = 2000$ (3.80%)	
	error	time (s)	error	time (s)	error	time (s)
nuclear	4.36 $\pm$ 0.03	2.1 $\pm$ 0.2	3.75 $\pm$ 0.03	4.2 $\pm$ 1.0	3.33 $\pm$ 0.01	40.9 $\pm$ 7.2
factored nuclear	2.46 $\pm$ 0.03	0.08 $\pm$ 0.02	2.18 $\pm$ 0.04	0.3 $\pm$ 0.1	1.98 $\pm$ 0.01	1.5 $\pm$ 0.2
BPMF	2.34 $\pm$ 0.05	3.2 $\pm$ 0.4	2.03 $\pm$ 0.05	5.8 $\pm$ 0.9	1.88 $\pm$ 0.01	48.3 $\pm$ 5.9
factored GSR	2.19 $\pm$ 0.03	0.5 $\pm$ 0.1	1.97 $\pm$ 0.04	4.2 $\pm$ 0.2	1.85 $\pm$ 0.01	6.7 $\pm$ 0.4
truncated $\ell_{1-2}$	<b>1.96<math>\pm</math>0.03</b>	695.8 $\pm$ 19.2	<b>1.82<math>\pm</math>0.04</b>	1083.2 $\pm$ 40.78	<b>1.77<math>\pm</math>0.01</b>	3954.1 $\pm$ 98.7
capped- $\ell_1$	<b>1.97<math>\pm</math>0.03</b>	0.8 $\pm$ 0.1	<b>1.83<math>\pm</math>0.03</b>	5.4 $\pm$ 0.1	<b>1.78<math>\pm</math>0.01</b>	36.0 $\pm$ 3.4
LSP	<b>1.97<math>\pm</math>0.03</b>	0.8 $\pm$ 0.1	<b>1.83<math>\pm</math>0.04</b>	5.1 $\pm$ 0.1	<b>1.77<math>\pm</math>0.01</b>	35.1 $\pm$ 2.1
MCP	<b>1.96<math>\pm</math>0.03</b>	0.7 $\pm$ 0.1	<b>1.82<math>\pm</math>0.03</b>	4.1 $\pm$ 0.2	<b>1.78<math>\pm</math>0.01</b>	40.6 $\pm$ 3.6
NNFN	<b>1.96<math>\pm</math>0.03</b>	2.1 $\pm$ 0.2	<b>1.82<math>\pm</math>0.03</b>	7.7 $\pm$ 0.6	<b>1.77<math>\pm</math>0.01</b>	43.1 $\pm$ 2.3
factored NNFN	<b>1.96<math>\pm</math>0.03</b>	<b>0.04<math>\pm</math>0.01</b>	<b>1.82<math>\pm</math>0.03</b>	<b>0.08<math>\pm</math>0.02</b>	<b>1.77<math>\pm</math>0.01</b>	<b>0.3<math>\pm</math>0.1</b>

Table 9: Performance on the recommendation and hyperspectral data. Error is RMSE scaled by  $10^{-1}$ . Entries marked as "-" mean that the corresponding methods cannot complete in three hours. The best and comparable results (according to the pairwise t-test with 95% confidence) are highlighted in bold.

	<i>MovieLens-1M</i>		<i>MovieLens-10M</i>		<i>Yahoo</i>	
	error	time (s)	error	time (s)	error	time (s)
nuclear	8.20 $\pm$ 0.02	118.7 $\pm$ 19.2	-	-	-	-
factored nuclear	8.10 $\pm$ 0.01	25.3 $\pm$ 3.7	7.95 $\pm$ 0.01	628.1 $\pm$ 24.2	7.10 $\pm$ 0.08	860.3 $\pm$ 33.1
BPMF	8.07 $\pm$ 0.01	215.3 $\pm$ 29.4	7.91 $\pm$ 0.01	819.6 $\pm$ 30.8	7.07 $\pm$ 0.03	1433.5 $\pm$ 89.2
factored GSR	8.05 $\pm$ 0.01	14.2 $\pm$ 1.5	-	-	-	-
truncated $\ell_{1-2}$	<b>7.97<math>\pm</math>0.01</b>	6068.4 $\pm$ 172.0	-	-	-	-
capped- $\ell_1$	8.00 $\pm$ 0.01	147.9 $\pm$ 23.3	7.87 $\pm$ 0.01	812.3 $\pm$ 29.7	6.58 $\pm$ 0.01	1296.8 $\pm$ 67.3
LSP	7.99 $\pm$ 0.01	149.2 $\pm$ 23.5	7.87 $\pm$ 0.01	850.8 $\pm$ 31.1	6.56 $\pm$ 0.01	1078.0 $\pm$ 69.0
MCP	8.01 $\pm$ 0.01	151.4 $\pm$ 23.9	7.87 $\pm$ 0.01	849.8 $\pm$ 31.5	6.78 $\pm$ 0.01	1108.3 $\pm$ 41.4
NNFN	<b>7.97<math>\pm</math>0.01</b>	134.2 $\pm$ 19.6	-	-	-	-
factored NNFN	<b>7.97<math>\pm</math>0.01</b>	<b>0.5<math>\pm</math>0.1</b>	<b>7.82<math>\pm</math>0.01</b>	<b>40.0<math>\pm</math>5.5</b>	<b>6.52<math>\pm</math>0.01</b>	<b>522.5<math>\pm</math>21.9</b>

Table 10: Performance on the hyperspectral data. Error is RMSE scaled by  $10^{-1}$ . Entries marked as “-” mean that the corresponding methods cannot complete in three hours. The best and comparable results (according to the pairwise t-test with 95% confidence) are highlighted in bold.

	<i>building</i>		<i>cabbage</i>	
	error	time (s)	error	time (s)
nuclear	0.56±0.01	277.1±12.1	0.53±0.01	133.7±2.1
factored nuclear	0.54±0.01	12.6±0.6	0.49±0.01	11.5±1.7
BPMF	0.53±0.01	370.5±7.3	0.49±0.01	183.6±6.2
factored GSR	0.52±0.01	59.5±1.9	0.48±0.01	68.6±2.0
truncated $\ell_{1-2}$	<b>0.50±0.01</b>	9836.1±470.4	<b>0.46±0.01</b>	6934.2±190.1
capped- $\ell_1$	<b>0.50±0.01</b>	264.8±4.6	<b>0.46±0.01</b>	79.2±3.2
LSP	<b>0.50±0.01</b>	274.4±25.4	<b>0.46±0.01</b>	150.5±3.1
MCP	<b>0.50±0.01</b>	266.7±9.8	<b>0.46±0.01</b>	144.2±2.9
NNFN	<b>0.50±0.01</b>	295.5±11.3	<b>0.46±0.01</b>	82.9±2.0
factored NNFN	<b>0.50±0.01</b>	<b>6.2±0.5</b>	<b>0.46±0.01</b>	<b>3.6±0.4</b>

Table 11: Performance on the climate data sets. Error is RMSE scaled by  $10^{-1}$ . The best and comparable results (according to the pairwise t-test with 95% confidence) are highlighted in bold.

	<i>GAS</i>				<i>USHCN</i>			
	<i>CO<sub>2</sub></i>		<i>H<sub>2</sub></i>		<i>temperature</i>		<i>precipitation</i>	
	error	time(s)	error	time(s)	error	time(s)	error	time(s)
nuclear	5.84 ±0.05	1.0 ±0.1	5.93 ±0.06	0.8 ±0.1	4.80 ±0.14	108.5 ±4.1	8.28 ±0.20	84.9 ±11.2
factored nuclear	5.65 ±0.06	0.17 ±0.02	5.74 ±0.05	0.19 ±0.03	4.83 ±0.16	15.7 ±2.4	8.23 ±0.18	33.3 ±1.7
BPMF	5.52 ±0.05	3.2 ±0.3	5.54 ±0.05	3.4 ±0.4	4.64 ±0.12	148.1 ±7.7	8.19 ±0.15	125.1 ±8.1
GRALS	5.65 ±0.06	0.7 ±0.1	5.78 ±0.05	0.4 ±0.1	4.98 ±0.15	37.2 ±1.9	8.18 ±0.16	49.6 ±2.8
truncated $\ell_{1-2}$	<b>5.30</b> <b>±0.07</b>	11.0 ±1.2	<b>5.31</b> <b>±0.05</b>	7.3 ±1.8	<b>4.44</b> <b>±0.13</b>	573.9 ±18.1	<b>8.06</b> <b>±0.14</b>	318.5 ±9.7
capped- $\ell_1$	5.33 ±0.03	0.6 ±0.1	<b>5.31</b> <b>±0.05</b>	0.7 ±0.2	4.50 ±0.14	108.5 ±10.5	<b>8.06</b> <b>±0.14</b>	87.2 ±6.2
LSP	5.37 ±0.08	1.2 ±0.1	5.40 ±0.07	1.3 ±0.2	4.48 ±0.10	133.3 ±7.7	<b>8.06</b> <b>±0.14</b>	105.8 ±7.4
MCP	<b>5.30</b> <b>±0.08</b>	1.0 ±0.1	5.34 ±0.06	0.5 ±0.1	<b>4.44</b> <b>±0.13</b>	92.5 ±6.1	<b>8.06</b> <b>±0.14</b>	85.2 ±7.3
NNFN	<b>5.30</b> <b>±0.08</b>	0.4 ±0.1	<b>5.31</b> <b>±0.05</b>	0.5 ±0.1	<b>4.44</b> <b>±0.12</b>	57.1 ±3.3	<b>8.06</b> <b>±0.14</b>	66.4 ±5.1
factored NNFN	<b>5.30</b> <b>±0.06</b>	<b>0.05</b> <b>±0.01</b>	<b>5.31</b> <b>±0.05</b>	<b>0.05</b> <b>±0.02</b>	<b>4.44</b> <b>±0.12</b>	<b>5.9</b> <b>±1.4</b>	<b>8.06</b> <b>±0.15</b>	<b>13.5</b> <b>±1.9</b>